Materials Science and Engineering C 75 (2017) 1–6

Contents lists available at ScienceDirect

Materials Science and Engineering C

journal homepage: www.elsevier.com/locate/msec

Biocompatibility study on Ni-free Ti-based and Zr-based bulk metallic glasses

T.H. Li [a,1], P.C. Wong [c,1], S.F. Chang [b,1], P.H. Tsai [a], J.S.C. Jang [a,b,*], J.C. Huang [d]

[a] Institute of Material Science and Engineering, National Central University, Taoyuan, Taiwan
[b] Department of Mechanical Engineering, National Central University, Taoyuan, Taiwan
[c] Department of Biomedical Engineering, National Yang-Ming University, Taipei, Taiwan
[d] Department of Materials and Optoelectronic Science, National Sun Yat-Sen University, Kaohsiung, Taiwan

ARTICLE INFO

Article history:
Received 14 September 2016
Received in revised form 15 November 2016
Accepted 3 February 2017
Available online 09 February 2017

Keywords:
Bulk metallic glass
L929 murine fibroblast cell line
MTT
Biocompatibility

ABSTRACT

Safety and reliability are crucial issues for medical instruments and implants. In the past few decays, bulk metallic glasses (BMGs) have drawn attentions due to their superior mechanical properties, good corrosion resistance, antibacterial and good biocompatibility. However, most Zr-based and Ti-based BMGs contain Ni as an important element which is prone to human allergy problem. In this study, the Ni-free Ti-based and Zr-based BMGs, $Ti_{40}Zr_{10}Cu_{36}Pd_{14}$, and $Zr_{48}Cu_{36}Al_8Ag_8$, were selected for systematical evaluation of their biocompatibility. Several biocompatibility tests, co-cultural with L929 murine fibroblast cell line, were carried out on these two BMGs, as well as the comparison samples of Ti6Al4V and pure Cu. The results in terms of cellular adhesion, cytotoxicity, and metallic ion release affection reveal that the $Ti_{40}Zr_{10}Cu_{36}Pd_{14}$ BMG and Ti6Al4V exhibit the optimum biocompatibility; cells still being attached on the petri dish with good adhesion and exhibiting the spindle shape after direct contact test. Furthermore, the $Ti_{40}Zr_{10}Cu_{36}Pd_{14}$ BMG showed very low Cu ion release level, in agreement with the MTT results. Based on the current findings, it is believed that Ni-free Ti-based BMG can act as an ideal candidate for medical implant.

1. Introduction

Metallic materials can be ideal biomaterials due to their enough mechanical properties and good formability. Therefore, metallic biomaterials were commonly used for load bearing medical devices, for example, orthopedic devices (bone screw, bone plate and artificial joint), dental devices (dental implant and dental brace), or cardiovascular stents or surgical instruments. Currently, the metal biomaterials in use are commonly stainless steel, Co-Cr-Mo alloy, and titanium alloy (such as Ti-6Al-4V or Ti-6Al-7Nb). These materials have been demonstrated to possess excellent biocompatibility and good corrosion resistance. Unfortunately, some of the physical and mechanical properties of these metallic implant materials do not match well with human bone (Table 1) [1–6], frequently causing the stress shielding effect and resulting in osteoporosis. Moreover, the wear debris generated from the metallic implant due to friction could induce osteolysis. Therefore, the safety and long-period stability of metallic materials are always crucial issues for implant in human body [5–11].

Bulk metallic glasses (BMGs) (also call bulk amorphous alloys) have attracted attention because of their special properties and microstructure. Compared with the traditional crystalline materials, the atomic configuration of the metallic glass lacks long-range order. This specific random atomic packing structure can offer higher strength (mainly owing to no dislocation), lower Young's modulus (owing to looser atomic packing) [12–15], higher corrosion resistant (due to no grain boundary) [16–19], higher wear resistant (due to high hardness) [20], excellent biocompatibility (when with right composition) [17–23], and antibacterial capability (when with Al or Ag) [24–26]. Therefore, BMGs may be another candidate for application for medical instruments and orthopedic implants. Recently, the Ni-free $Ti_{40}Zr_{10}Cu_{36}Pd_{14}$ BMG with relatively good glass forming ability (GFA) has been developed [12]. This BMG possesses yield strength of 1950 MPa and yield strain of 2.3%, promising for biomedical implant applications.

In order to systematically assess the biocompatibility of such Ni-free BMGs, two nickel-free $Ti_{40}Zr_{10}Cu_{36}Pd_{14}$ and $Zr_{48}Cu_{36}Al_8Ag_8$ BMGs were selected for detailed investigation. Three comparison metals, Ti6Al4V alloy, pure Cu, and pure Zr, are also examined concurrently according to ISO10993-5 (Biological evaluation of medical devices) [25]. The tests were divided into direct contact and indirect contact (MTT assay). In addition, the relationship between cell viability and the values of metallic ions release from samples, as well as the cell adhesion morphologies, were also investigated.

* Corresponding author.
E-mail address: jscjang@ncu.edu.tw (J.S.C. Jang).
[1] Authors with equal contribution.

http://dx.doi.org/10.1016/j.msec.2017.02.006
0928-4931/

Table 1
The physical and mechanical properties of various implant materials.

Properties	Natural bone	Ti alloy	Co-Cr alloy	Stainless steel	Ti-based BMG	Zr-based BMG
Density (g/cm^3)	1.8–2.1	4.4–4.5	8.3–9.2	7.9–8.1	4.4–5.2	5.9–6.7
Young's modulus (GPa)	3–20	110–117	230	189–205	78–115	80–100
Compressive yield strength (MPa)	130–180	758–1117	450–1000	170–310	1950–2165	~2000
Fracture toughness (MPa m$^{1/2}$)	3–6	55–115	N/A	50–200	40–100	50–90

2. Experimental procedures

2.1. Sample preparation and microstructure analyses

The alloy ingots based on the atomic compositions (at%) of $Ti_{40}Zr_{10}Cu_{36}Pd_{14}$ and $Zr_{48}Cu_{36}Al_8Ag_8$ were prepared by arc-melting of the appropriate mixture of high purity elements (>99.9 wt%) under a Ti-gettered argon atmosphere. The melting processes were repeated four times to ensure the homogeneity of ingot ingredients. Then the alloy ingots were remelted by arc-melting under a purified argon atmosphere. After complete melting, the liquid alloy was suction cast into a water-cooled Cu mold to form alloy plates with dimension of 40 mm in length × 10 mm in width × 2 mm in thickness. The samples were then cut into 10 mm^2 square by wire electrical discharge machining (EDM) and fine-polished for their 6 surfaces to make sure the flat surface roughness, which was measured by atomic force microscopy (Bruker DI3100 AFM) operated by the contact mode with a Si_3N_4 probe and a load <100 nN. The amorphous states of samples were examined by X-ray diffractometry (XRD, BRUKER, D8A XRD, Germany) with monochromatic Cu-Kα radiation. The chemical compositions of samples were analyzed by energy dispersive spectroscopy (EDS, FEI, Inspect F50, US), attached with scanning electron microscopy (SEM, FEI-Inspect F50, US), to confirm their compositions as originally designed.

2.2. Biocompatibility test

The mouse fibroblast cell line (L929) was used to examine the biocompatibility of the $Ti_{40}Zr_{10}Cu_{36}Pd_{14}$ BMG, $Zr_{48}Cu_{36}Al_8Ag_8$ BMG, commercial Ti6Al4V alloy, pure Cu (negative control), and pure Zr (positive control) in this study. L929 cells were cultured in Dulbecco's modified Eagle medium (DMEM) and 10% fetal bovine serum (FBS). The biocompatibility tests were executed by the direct contact and indirect contact methods. All the biocompatibility tests were conducted three times to ensure repeatability.

2.2.1. Cell adhesion observation

The cell morphologies adhered on sample surfaces were observed by SEM. The samples with a dimension of 10 mm × 10 mm × 2 mm were cleaned by ultrasound cleaner after polishing. This cell adhesion experiment was conducted following the procedures below. (1) The 75% ethanol was used to immerse the samples to make sure that the samples were sterile. (2) The samples were co-cultured with cells in 1 ml of cell suspension (5×10^4 cell/ml) in a 24-well culture plates. (3) After 48-hour culturing, until the cells attached to the samples, the medium was removed and each well was rinsed by 0.1 M phosphate-buffered saline (PBS). Then, the 500 μl 4% formaldehyde was added to the well to play the role of fixation. (4) After 2 h, the formaldehyde removal and cellular dehydration treatment were carried out with different concentrations of ethanol. (5) The critical point dry method was applied to dehydrate the samples before it is sent into the SEM chamber, then the morphologies of cells were observation by SEM.

2.2.2. Direct contact

For the direct contact method in this study, $Ti_{40}Zr_{10}Cu_{36}Pd_{14}$ BMG, $Zr_{48}Cu_{36}Al_8Ag_8$ BMG, Ti6Al4V alloy, pure Cu, and pure Zr were used to contact with cells directly. Firstly, the samples were co-cultured with cells in 2 ml/well of cell suspension (5×10^4 cells/ml) in a 23-well culture plate and cultured in the incubator with 37 °C and 5% CO_2 atmosphere for 48 h. Secondly, all samples were put on the cells after surface cleaning and cultured in the incubator with 37 °C and 5% CO_2 atmosphere for another 24 h. Finally, the cell morphology was observed by optical microscopy (OM, OLYMPUS-CKX41, Japan).

2.2.3. Indirect contact

In this method, a precipitate medium was extracted from the DMEM immersed with the $Ti_{40}Zr_{10}Cu_{36}Pd_{14}$ BMG, $Zr_{48}Cu_{36}Al_8Ag_8$ BMG, Ti6Al4V alloy, and pure Cu, and pure Zr at different time periods (Day 1, 3, and 5). The samples were co-cultured with 100 μl of cell suspension (1×10^4 cells/well) in a 96-well culture plate and cultured in the incubator with 37 °C and 5% CO_2 atmosphere in another 24 h. According to ISO10993-12 [27], the volume of culture medium can be calculated by the dimension of sample (10 mm × 10 mm × 2 mm), 0.667 ml. Finally, 50 μl/well of 3-(4,5-dimethylthiazol-2-yl)-2,5-diphenyltetrazolium bromide (MTT solution) was added to each well carefully and incubated the plates at 37 °C and 5% CO_2 atmosphere. After 2 h, 100 μl Isopropanol was added and the optical density (OD) values can be read over the wavelength of 560 nm by the Enzyme-linked Immuno-sorbent Assay (ELISA) reader. The extraction medium was distilled and analyzed for its concentration of metallic ions by inductively coupled plasma-mass spectrometer (ICP-MS, Agilent 7500ce, Japan).

3. Results and discussion

The EDS results revealed that the measured chemical compositions of $Ti_{40}Zr_{10}Cu_{36}Pd_{14}$ and $Zr_{48}Cu_{36}Al_8Ag_8$ plates are close to their pre-set readings, as listed in Table 2. The XRD patterns of these two BMGs present a typical amorphous nature with a diffuse hump around 30° ~ 50° and no apparent crystalline peak, as shown in Fig. 1. After standard polishing, the average surface roughness Ra readings, measured by atomic force microscope (AFM), of the as-polished $Ti_{40}Zr_{10}Cu_{36}Pd_{14}$ BMG, $Zr_{48}Cu_{36}Al_8Ag_8$ BMG, and Ti6Al4V alloy exhibit similar values, around 2.0–3.5 nm, as some illustrated in Fig. 2. According to the literature report, the rough surface can promote the attachment and differentiation of bone cells [28,29], but the smooth surface is favorable for the

Table 2
Chemical compositions of $Ti_{40}Zr_{10}Cu_{36}Pd_{14}$ BMG and $Zr_{48}Cu_{36}Al_8Ag_8$ BMG analyzed by EDS.

		Ti	Zr	Cu	Pd
$Ti_{40}Zr_{10}Cu_{36}Pd_{14}$	Preset (at%)	40	10	36	14
	Analyzed (at%)	41.7	8.9	38.3	11.1
		Zr	Cu	Al	Ag
$Zr_{48}Cu_{36}Al_8Ag_8$	Preset (at%)	48	36	8	8
	Analyzed (at%)	48.9	36.1	7.7	7.3

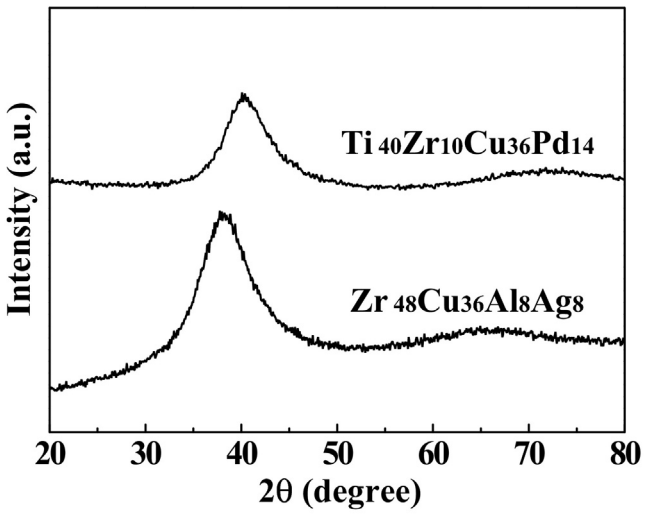

Fig. 1. XRD patterns of the $Ti_{40}Zr_{10}Cu_{36}Pd_{14}$ BMG and $Zr_{48}Cu_{36}Al_8Ag_8$ BMG.

attachment and differentiation of fibroblast [30]. Therefore, it is expected that all of the samples of $Ti_{40}Zr_{10}Cu_{36}Pd_{14}$ BMG, $Zr_{48}Cu_{36}Al_8Ag_8$ BMG, Ti6Al4V alloy, pure Cu and pure Zr will stand at the same base condition for the cell adhesion test.

After 48 hours culturing, the anchorage-dependent cells (L929 cell line) on the surface of $Ti_{40}Zr_{10}Cu_{36}Pd_{14}$ BMG, $Zr_{48}Cu_{36}Al_8Ag_8$ BMG, Ti6Al4V alloy, pure Cu and pure Zr, the morphologies of cell adhesion characterized by SEM are illustrated in Fig. 3. Both of the health L929 cells that cultured on the surface of $Ti_{40}Zr_{10}Cu_{36}Pd_{14}$ BMG, Ti6Al4V alloy, and pure Zr show a very well spread and extended morphology, a spindle shape accompanied with filopodium which is similar to the cell morphology of blank control. However, the L929 cells on $Zr_{48}Cu_{36}Al_8Ag_8$ BMG present a totally different morphology and looks like apoptosis. This may be caused by the increase in local concentration of Cu ion that release from the $Zr_{48}Cu_{36}Al_8Ag_8$ BMG and will be discussed in the ICP analysis. Moreover, more cells in number were found to attach on the surface of $Ti_{40}Zr_{10}Cu_{36}Pd_{14}$ BMG than those on the surface of Ti6Al4V alloy. Eisenbarth et al. [31] have reported that the cells may lead to a decrease in adhesion on the Ti6Al4V alloy after 14 days culture time due to an increase in local concentration of vanadium ions released from the Ti6Al4V alloy after longer incubation time. Therefore, the cells adhesion behavior not only depends on the surface roughness but also depends on the type and concentration of ions released from the material.

In the direct contact test, after 24 hours culturing, the metallic ions were released to the culture medium and contact with cells. The cell growth degrees on the five specimens ($Ti_{40}Zr_{10}Cu_{36}Pd_{14}$ BMG, $Zr_{48}Cu_{36}Al_8Ag_8$ BMG, Ti6Al4V alloy, pure Cu, and pure Zr) were revealed by this direct contact test. It appeared that the L929 cells were totally killed in the culture environment of pure Cu (negative control) due to its very high concentration of Cu ions released from the pure Cu substrate during the culturing and poison the cell [32]. Meanwhile, only small portion of cells can survive in the culture environment of the $Zr_{48}Cu_{36}Al_8Ag_8$ BMG. Conversely, the L929 cells can entirely survive in the environments of the $Ti_{40}Zr_{10}Cu_{36}Pd_{14}$ BMG and Ti6Al4V alloy, as illustrated in Fig. 4 (top view) and Fig. 5 (bottom view). The large differences on the results of direct contact test between the $Ti_{40}Zr_{10}Cu_{36}Pd_{14}$ BMG and $Zr_{48}Cu_{36}Al_8Ag_8$ are suggested due to the different releasing rates of cu ion in the culture media between these two BMGs, and will be explained by the ICP results later. In summary, according to the ISO 10993-5 [27], $Ti_{40}Zr_{10}Cu_{36}Pd_{14}$ BMG can be classified to the first level (slight cytotoxicity) which is the same level as Ti6Al4V alloy and pure Zr, but $Zr_{48}Cu_{36}Al_8Ag_8$ BMG and pure Cu would be classified to the fourth level (severely cytotoxicity).

Fig. 6 shows the quantitative viability of L929 cell cultured in the extraction medium with the $Ti_{40}Zr_{10}Cu_{36}Pd_{14}$ BMG, $Zr_{48}Cu_{36}Al_8Ag_8$ BMG, Ti6Al4V alloy, pure Cu, and pure Zr, and the cell viability were

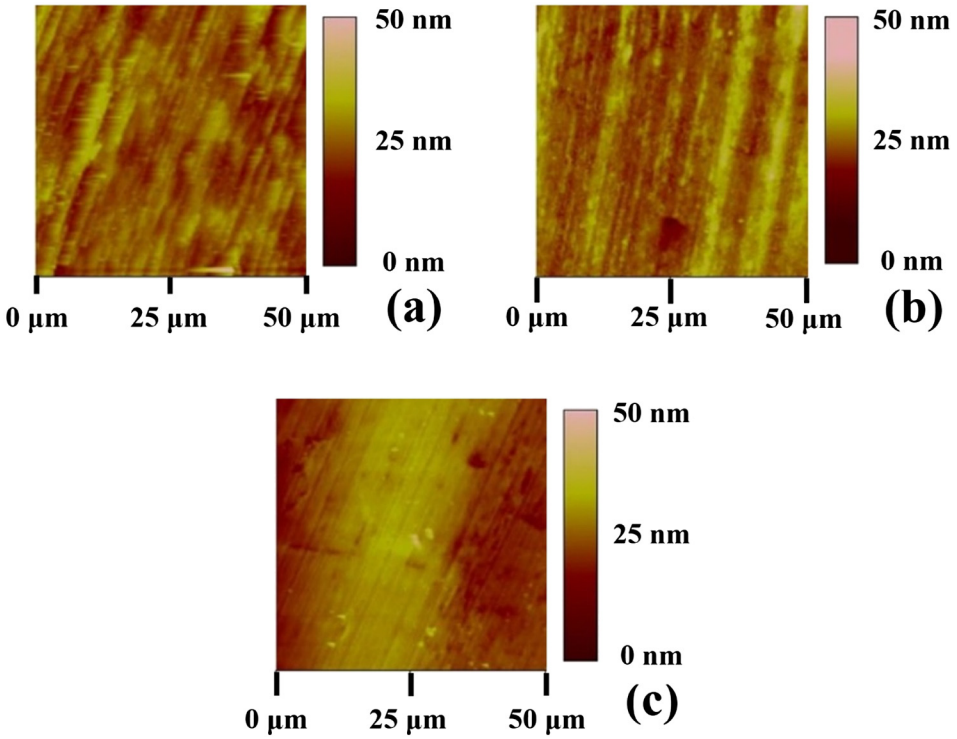

Fig. 2. AFM images of surface morphology of the as-polished (a) $Ti_{40}Zr_{10}Cu_{36}Pd_{14}$ BMG, $Zr_{48}Cu_{36}Al_8Ag_8$ BMG and (c) Ti6Al4V alloy.

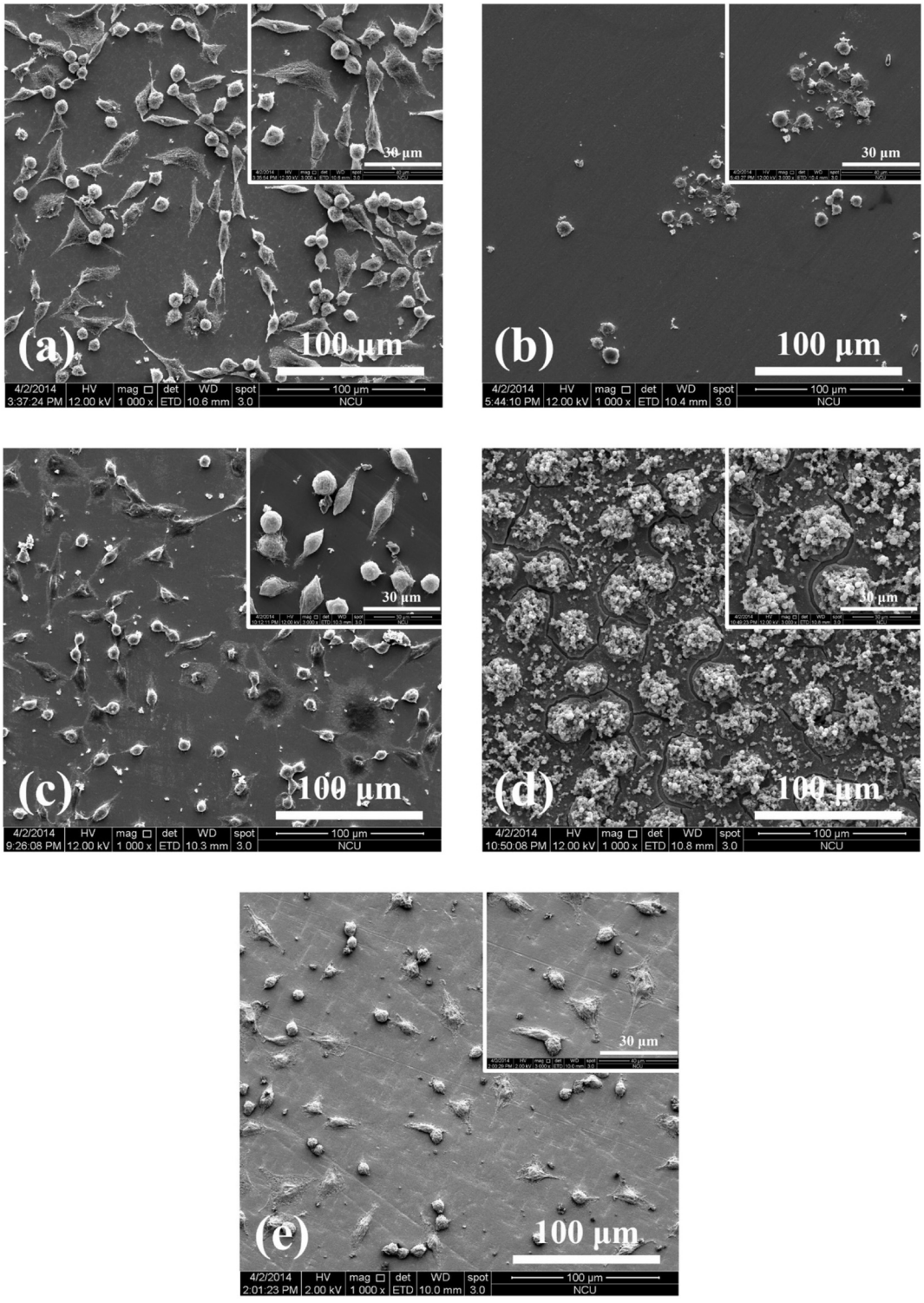

Fig. 3. SEM images of cell adhesion on the surface of (a) $Ti_{40}Zr_{10}Cu_{36}Pd_{14}$ BMG, (b) $Zr_{48}Cu_{36}Al_8Ag_8$ BMG, (c) Ti6Al4V alloy, (d) pure Cu, and (e) pure Zr. The enlarged image is located at the up-right corner of each figure, respectively.

normalized with blank group. On the first day, the cell viability in the extracts of $Ti_{40}Zr_{10}Cu_{36}Pd_{14}$ BMG and Ti6Al4V alloy groups presented slightly lower percentage values than that of the blank group. However, until day 5, both of the cell viability in the extracts of $Ti_{40}Zr_{10}Cu_{36}Pd_{14}$ BMG and Ti6Al4V alloy exhibited higher percentage values than that of the blank group. This result indicates that the lower viability values at initial contact between cells and metallic ions was caused by the cell maladjustment, then the cells would adapt to the environment gradually until day 5. In general, both of $Ti_{40}Zr_{10}Cu_{36}Pd_{14}$ BMG and Ti6Al4V alloy groups show similar result in biocompatibility test with >90% viability that is even better than the cell viability of pure Zr group (positive). On the contrary, the cell viability of $Zr_{48}Cu_{36}Al_8Ag_8$ BMG and pure Cu groups are <30% after 5 days culturing. This means that both $Zr_{48}Cu_{36}Al_8Ag_8$ BMG and pure Cu have apparent cytotoxicity effects on the L929 cell.

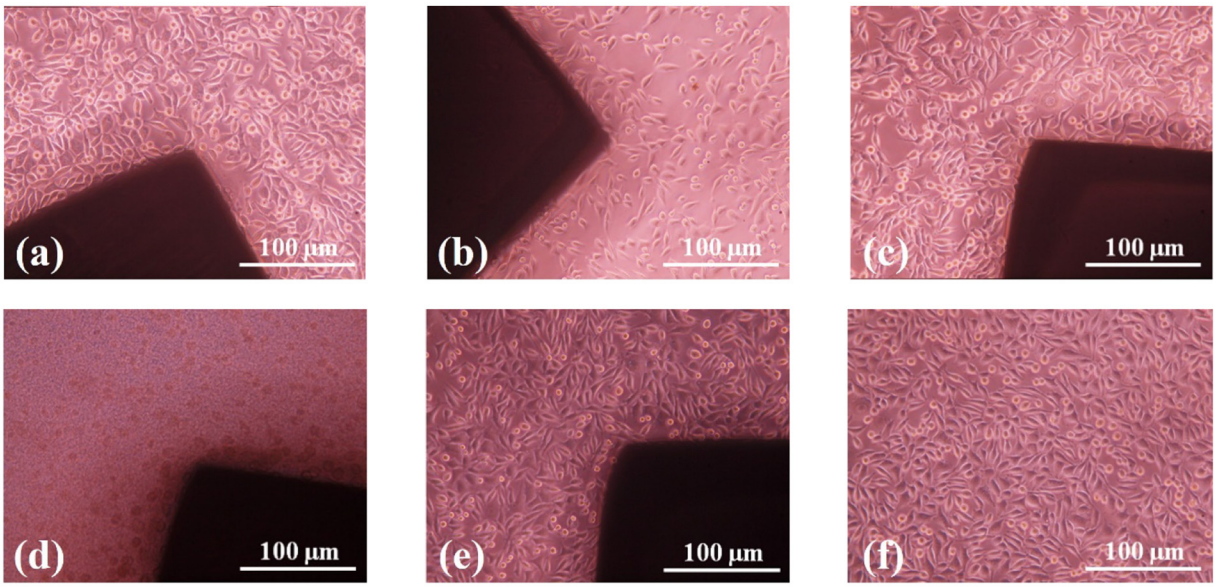

Fig. 4. The situation of L929 cells around the sample (top view): (a) $Ti_{40}Zr_{10}Cu_{36}Pd_{14}$ BMG, (b) $Zr_{48}Cu_{36}Al_8Ag_8$ BMG, (c) Ti6Al4V, (d) Pure Cu (negative), (e) Pure Zr (positive), (f) Blank (control).

Finally, the ICP-MS ion release analyses are illustrated in Fig. 7 for the extraction medium of both the $Ti_{40}Zr_{10}Cu_{36}Pd_{14}$ and $Zr_{48}Cu_{36}Al_8Ag_8$ BMGs, after immersion for 1, 3, and 5 days. From Fig. 7, it can be seen that the $Ti_{40}Zr_{10}Cu_{36}Pd_{14}$ BMG basically only release very small amount of Cu ions (<3600 ppb even after 5 days). The strong atomic mutual bonding from Ti/Zr/Pd atoms attracting the Cu atoms (due to negative heat of mixing) would create strong resistance from Cu to be released. This effect imposes the positive biocompatibility response of the $Ti_{40}Zr_{10}Cu_{36}Pd_{14}$ BMG, even with 36% Cu content in the glass. In contrast, the Cu ion release from the $Zr_{48}Cu_{36}Al_8Ag_8$ BMG is significantly higher in Fig. 7, >20.000 ppb after 1 day, and even 80,000 ppb after 3 days culturing. In addition, note that there are other ion releases, including Al, Zr, and Ag ions. For example, the Ag ion release can be as high as 40,000 ppb after 5 days. The atomic mutual bonding in this $Zr_{48}Cu_{36}Al_8Ag_8$ BMG is much weaker. It follows that the combined severer ion releases from Cu, Al, Zr, and Ag together would result in the inferior cell viability for the $Zr_{48}Cu_{36}Al_8Ag_8$ BMG. This is in good agreement with the indirect contact (MTT) results.

4. Conclusion

Based on the results of biocompatibility test, the following conclusions can be drawn.

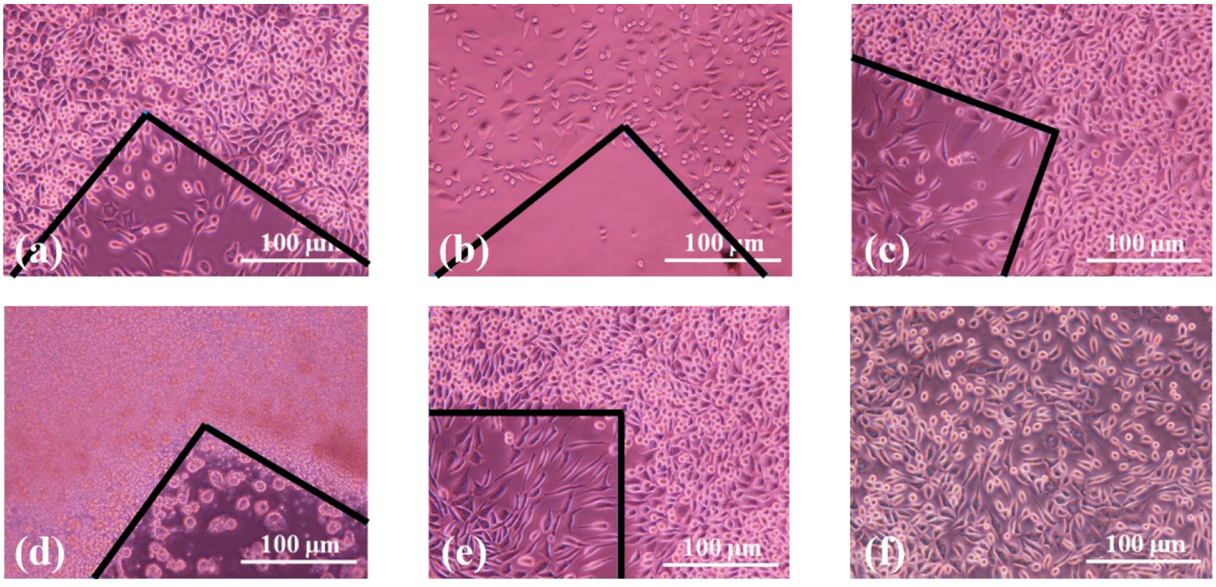

Fig. 5. The situation of L929 cells around the sample (bottom view): (a) $Ti_{40}Zr_{10}Cu_{36}Pd_{14}$ BMG, (b) $Zr_{48}Cu_{36}Al_8Ag_8$ BMG, (c) Ti6Al4V, (d) Pure Cu (negative), (e) Pure Zr (positive), (f) Blank (control).

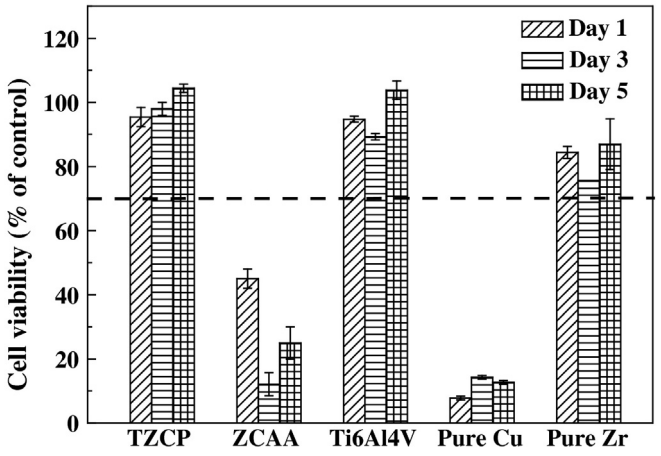

Fig. 6. Cell cytotoxicity of L929 cells cultured in the extraction medium from $Ti_{40}Zr_{10}Cu_{36}Pd_{14}$ BMG (TZCP), $Zr_{48}Cu_{36}Al_8Ag_8$ BMG (ZCAA), Ti6Al4V alloy, Pure Cu, and Pure Zr groups, respectively were normalized to the same control. Note that reduction of cell viability by >30% (dash line) is considered a cytotoxic effect.

1. Both the $Ti_{40}Zr_{10}Cu_{36}Pd_{14}$ BMG and Ti6Al4V alloy present similar cell adhesion behavior after 48 hours culturing, the health L929 cells show a very well spread and extended morphology with a spindle shape filopodium. Moreover, more cell numbers were found to attach on the surface of $Ti_{40}Zr_{10}Cu_{36}Pd_{14}$ BMG than that on the surface of Ti6Al4V alloy.
2. The cell survival rate of $Ti_{40}Zr_{10}Cu_{36}Pd_{14}$ BMG and Ti6Al4V alloy can reach to 99% ± 5% by direct as well as indirect contact tests. According to ISO 10993-5, $Ti_{40}Zr_{10}Cu_{36}Pd_{14}$ BMG can be classified to the first level (slight cytotoxicity) which is the same level as Ti6Al4V alloy, but $Zr_{48}Cu_{36}Al_8Ag_8$ BMG would be classified to the fourth level (severely cytotoxicity).
3. In summary, the $Ti_{40}Zr_{10}Cu_{36}Pd_{14}$ BMG is believed to have great potential in medical field due to its excellent biocompatibility similar to or even better than the Ti6Al4V alloy.

Acknowledgement

The authors would like to gratefully acknowledge the sponsorship from the Ministry of Science and Technology of Republic of China under the project of NSC101-2221-E-008-043-MY3 and MOST103-2120-M-110-004.

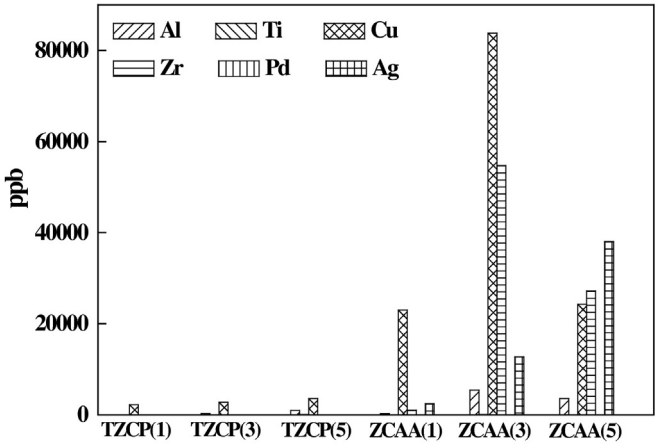

Fig. 7. Metallic ion concentration of extraction medium from $Ti_{40}Zr_{10}Cu_{36}Pd_{14}$ BMG (TZCP) and $Zr_{48}Cu_{36}Al_8Ag_8$ BMG (ZCAA) at different time periods.

References

[1] P.E. DeGarmo, Materials and Processes in Manufacturing, Fifth ed. Collin Macmillan, New York, 1979.
[2] L. Gibson, M. Ashby, Cellular Solids - Structure and Properties, Sydney, 1988 1–41.
[3] L. Gibson, M. Ashby, Cellular Solids - Structure and Properties, Sydney, 1988 316–331.
[4] M.P. Staiger, A.M. Pietak, J. Huadmai, G. Dias, Magnesium and its alloys as orthopedic biomaterials: a review, Biomaterials 27 (2006) 1718–1734.
[5] X.J. Gua, S.J. Poon, G.J. Shiflet, J.J. Lewandowski, Compressive plasticity and toughness of a Ti-based bulk metallic glass, Acta Mater. 58 (2010) 1708–1720.
[6] Y.S. Chang, K.T. Hsu, J.B. Li, P.H. Tsai, J.S.C. Jang, J.C. Huang, Effect of cast process and microalloying on the fracture toughness of Zr-based bulk amorphous alloys, J. Alloys Compd. 614 (2014) 87–93.
[7] M. Niinomi, Metals for Biomedical devices, First ed. Woodhead Publishing, 2010.
[8] C. Leyens, M. Peters, Titanium and Titanium Alloys: Fundamentals and Applications, Wiley, Weinheim, 2003.
[9] B. Basu, D. Katti, A. Kumar, Advanced Biomaterials-Fundamentals, Processing, and Applications, Wiley, Weinheim, 2009.
[10] M. Geetha, A.K. Singh, R. Asokamani, A.K. Gogia, Ti based biomaterials, the ultimate choice for orthopaedic implants - a review, Prog. Mater. Sci. 54 (2009) 397–425.
[11] M. Long, H.J. Rack, Titanium alloys in total joint replacement-a materials science perspective, Biomaterials 19 (1998) 1621–1639.
[12] S.L. Zhu, X.M. Wang, F.X. Qin, A. Inoue, A new Ti-based bulk glassy alloy with potential for biomedical application, Mater. Sci. Eng. A 459 (2007) 223–237.
[13] J.J. Oak, A. Inoue, Attempt to develop Ti-based amorphous alloys for biomaterials, Mater. Sci. Eng. A 449-451 (2007) 220–224.
[14] Z. Liu, L. Huang, W. Wu, X. Luo, M. Shi, P.K. Liaw, W. He, T. Zhang, Novel low Cu content and Ni-free Zr-based bulk metallic glasses for biomedical applications, J. Non-Cryst. Solids 363 (2013) 1–5.
[15] L. Liu, C.L. Qiu, C.Y. Huang, Y. Yu, H. Huang, S.M. Zhang, Biocompatibility of Ni-free Zr-based bulk metallic glasses, Intermetallics 17 (2009) 235–240.
[16] C.L. Qiu, Q. Chen, L. Liu, K.C. Chan, J.X. Zhou, P.P. Chen, S.M. Zhang, A novel Ni-free Zr-based bulk metallic glass with enhanced plasticity and good biocompatibility, Scr. Mater. 55 (2006) 605–608.
[17] H.H. Huang, Y.S. Sun, C.P. Wu, C.F. Liu, P.K. Liaw, W. Kai, Corrosion resistance and biocompatibility of Ni-free Zr-based bulk metallic glass for biomedical applications, Intermetallics 30 (2012) 139–143.
[18] N. Hua, L. Huang, J. Wang, Y. Cao, W. He, S. Pang, T. Zhang, Corrosion behavior and in vitro biocompatibility of Zr-Al-Co-Ag bulk metallic glasses: an experimental case study, J. Non-Cryst. Solids 358 (2012) 1599–1604.
[19] Z. Liu, L. Huang, W. Wu, X. Luo, M. Shi, P.K. Liaw, W. He, T. Zhang, Novel low Cu content and Ni-free Zr-based bulk metallic glasses for biomedical applications, J. Non-Cryst. Solids 363 (2013) 1–5.
[20] L. Liu, C.L. Qiu, C.Y. Huang, Y. Yu, H. Huang, S.M. Zhang, Biocompatibility of Ni-free Zr-based bulk metallic glasses, Intermetallics 17 (2009) 235–240.
[21] H.F. Li, Y.F. Zheng, F. Xu, J.Z. Jiang, In vitro investigation of novel Ni free Zr-based bulk metallic glasses as potential biomaterials, Mater. Lett. 75 (2012) 74–76.
[22] C.H. Lin, C.H. Huang, J.F. Chuang, J.C. Huang, J.S.C. Jang, C.H. Chen, Rapid screening of potential metallic glasses for biomedical applications, Mater. Sci. Eng. C 33 (2013) 4520–4526.
[23] C.H. Lin, C.H. Huang, J.F. Chuang, J.C. Huang, J.S.C. Jang, C.H. Chen, Electrochemical and biocompatibility response of newly developed TiZr-based metallic glasses, Mater. Sci. Eng. C 43 (2014) 343–349.
[24] P.T. Chiang, G.J. Chen, S.R. Jian, Y.H. Shih, J.S.C. Jang, C.H. Lai, Surface antimicrobial capabilities of the ZrAlNiCuSi metallic glass thin film for *Escherichia coli*, *Staphylococcus aureus*, *Pseudomonas aeruginosa*, *Acinetobacter baumannii* and *Candida albicans*, FJHS 2 (2010) 12–20.
[25] H.W. Chen, K.C. Hsu, Y.C. Chan, J.G. Duh, J.W. Lee, J.S.C. Jang, G.J. Chen, Antimicrobial properties of Zr-Cu-Al-Ag thin film metallic glass, Thin Solid Films 561 (2014) 98–101.
[26] J.P. Chu, T.Y. Liu, C.L. Li, C.H. Wang, J.S.C. Jang, M.J. Chen, S.H. Chang, W.C. Huang, Fabrication and characterizations of thin film metallic glasses: antibacterial property and durability study for medical application, Thin Solid Films 561 (2014) 98–101.
[27] International Organization for Standardization, ISO-10993: Biological Evaluation of Medical Devices, third ed., 2003.
[28] K. Kieswetter, Z. Schwartz, D.D. Dean, B.D. Boyan, The role of implant surface characteristics in the healing of bone, Crit. Rev. Oral Biol. Med. 7 (1996) 329–345.
[29] B.D. Boyan, T.W. Hummert, D.D. Dean, Z. Schwartz, Role of material surfaces in regulating bone and cartilage cell response, Biomaterials 17 (1996) 137–146.
[30] K. Rornu, W.J. Malomey, M.A. Kelly, R.L. Smith, Osteoblast adhesion to orthopaedic implant alloy: effects of cell adhesion molecules and diamond-like carbon coating, J. Orthop. Res. 14 (1996) 871–877.
[31] E. Eisenbarth, J. Meyle, W. Nachtigall, J. Breme, Influence of the surface structure of titanium materials on the adhesion of fibroblast, Biomaterials 17 (1996) 1399–1403.
[32] M.E. Letelier, A.M. Lepe, M. Faundez, J. Salazai, R. Marin, P. Aracena, H. Speisky, Possible mechanisms underlying copper-induced damage in biological membranes leading to cellular toxicity, Chem. Biol. Interact. 151 (2005) 71–82.